

See discussions, stats, and author profiles for this publication at: <https://www.researchgate.net/publication/51781273>

Stereochemical Dependence of $(3)J(\text{CH})$ Coupling Constants in 2-Substituted 4-*t*-Butyl-cyclohexanone and Their Alcohol Derivatives

ARTICLE *in* THE JOURNAL OF PHYSICAL CHEMISTRY A · NOVEMBER 2011

Impact Factor: 2.69 · DOI: 10.1021/jp2083456 · Source: PubMed

CITATIONS

2

READS

33

5 AUTHORS, INCLUDING:



Denize Cristina Favaro

University of São Paulo

9 PUBLICATIONS 33 CITATIONS

[SEE PROFILE](#)



Lucas C Ducati

University of São Paulo

41 PUBLICATIONS 211 CITATIONS

[SEE PROFILE](#)



Rubén H Contreras

University of Buenos Aires

201 PUBLICATIONS 2,995 CITATIONS

[SEE PROFILE](#)



Claudio Tormena

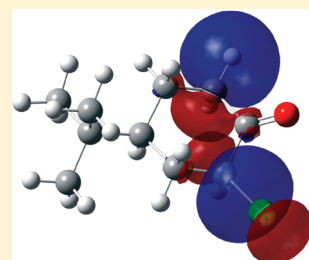
University of Campinas

144 PUBLICATIONS 1,261 CITATIONS

[SEE PROFILE](#)

Stereochemical Dependence of $^3J_{\text{CH}}$ Coupling Constants in 2-Substituted 4-*t*-Butyl-cyclohexanone and Their Alcohol DerivativesDenize C. Favaro,[†] Lucas C. Ducati,[†] Francisco P. dos Santos,[†] Rubén H. Contreras,[‡] and Cláudio F. Tormena^{*,†}[†]Chemistry Institute, State University of Campinas, Caixa Postal 6154, 13084-971 Campinas SP, Brazil[‡]Department of Physics, FCEyN, University of Buenos Aires and IFIBA-CONICET, Buenos Aires, Argentina

ABSTRACT: Theoretical and experimental studies on $^3J_{\text{C2H6eq}}$ NMR spin–spin coupling constants in both the 2-*X*-4-*t*-butyl-cyclohexanone (*X* = H, CH₃, F, Cl, and Br) and in their alcohol derivatives series are reported. Results thus found are rationalized in terms of the transmission of the Fermi contact contribution to such couplings. To this end, dependencies of $^3J_{\text{C2H6eq}}$ couplings versus the C₂–C₁–C₆ angle are compared in both series for equatorial and axial *X* orientations. The main trend is described in terms of the rear lobes interaction. Besides, for *X* = halogen atom in equatorial orientation a rather strong interaction between oxygen and halogen lone pairs is observed, and its influence on $^3J_{\text{C2H6eq}}$ couplings is discussed and rationalized in terms of different Fermi contact transmission pathways.



■ INTRODUCTION

Since the early work by Karplus,^{1–3} vicinal $^3J_{\text{HH}}$ indirect spin–spin coupling constants, SSCCs, were extensively studied, and many experimental and theoretical works have been published in which several effects affecting the original Karplus relationship were discussed.⁴ Besides $^3J_{\text{HH}}$ SSCCs, other vicinal heteronuclear SSCCs like $^3J_{\text{CH}}$ SSCCs are also of importance in many areas of structural chemistry like, for instance, for studying constitutions, configurations, and conformations in organic and bioorganic molecules, mainly when other parameters such as $^3J_{\text{HH}}$ SSCCs and NOE experiments are inconclusive.^{5–8} Both types of SSCCs, $^3J_{\text{HH}}$ and $^3J_{\text{CH}}$, seem to be similarly affected by factors such as substituent effects,^{9,10} substituent orientation,¹¹ bond angles along the coupling pathway,^{12,13} the presence of a heteroatom along the coupling pathway,^{14,15} and hyperconjugative interactions involving bonding or antibonding orbitals belonging to the coupling pathway. Such works were aimed at studying how different factors affect contributions from the three bonds connecting both coupling nuclei. During the past few years it was concluded that not only long-range couplings could be transmitted through several pathways but also vicinal^{16–18} and even geminal¹⁹ SSCCs can be transmitted through more than one coupling pathway, which could lead to quite an unusual value of coupling constant. This possibility is also explored in this work.

Parella et al.⁵ have reported that in 4-*t*-butylcyclohexanone, compound **1** (Scheme 1), three-bond J_{CH} SSCCs across the carbonyl group have an unusually small value, like, for instance, $^3J_{\text{C6H2eq}} = 3.1$ Hz corresponding to a pathway with the C₆–C₁–C₂–H_{2eq} dihedral angle of 173.9°. This contrasts notably with $^3J_{\text{C1H3eq}} = 8.4$ Hz for a 176.9° C₁–C₂–C₃–H_{3eq} dihedral angle measured in the same compound.²⁰ Similar effect was reported many years ago when considering that $^3J_{\text{C2H6}}$ SSCC is an adequate probe to discriminate between pyridine and pyridone

structures.²¹ Besides, in compound **1** for smaller C₆–C₁–C₂ angles the strain of the corresponding C₆–C₁ and C₁–C₂ bonds increase, favoring hyperconjugative interactions of type $\sigma_{\text{C1–C2}} \rightarrow \sigma^*_{\text{C6–H6eq}}$, which in turn favors the transmission of the FC term of $^3J_{\text{C6H2eq}}$, as observed in $^3J_{\text{C1H3}}$ SSCCs in 1-*X*-bicyclo[1.1.1]pentanes.¹⁶

In this work, we focus our attention on measuring and rationalizing the difference in $^3J_{\text{C2H6eq}}$ SSCCs when compound **1** is *X*-substituted (*X* = H, Me, F, Cl, and Br) at the ring position 2, both for equatorial (*cis*) (compounds **2a–5a**) and axial (*trans*) (compounds **2b–5b**) orientations. For completeness sake, a similar study is carried out on the analogous 2-*X*-4-*t*-butylcyclohexanols (*X* = H, Me, F, Cl, and Br) (compounds **6a** to **10d**); Scheme 1.

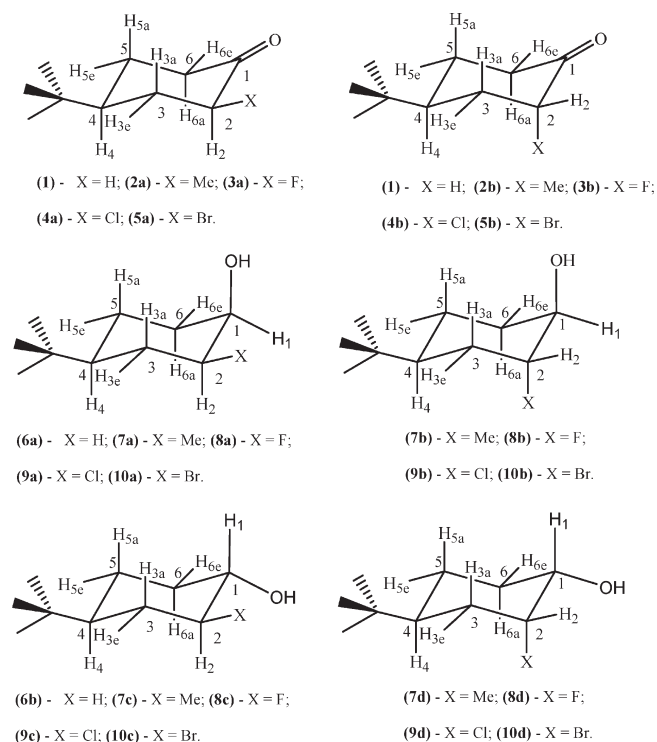
■ EXPERIMENTAL SECTION

$^3J_{\text{CH}}$ couplings were measured using the HSQC-TOCSY-IPAP pulse sequence²² on a Bruker Avance III 400 spectrometer equipped with an inverse 5 mm probe with *z*-gradient operating at 400.13 and 100.62 MHz for ¹H and ¹³C, respectively. Samples were prepared as solutions of 15 mg of solute in 0.7 mL of CDCl₃. Spectra were taken at 300 K. $^3J_{\text{CH}}$ SSCCs in compounds **1** to **10** (Scheme 1) were calculated using the CP/DFT framework²³ using the Gaussian03 package of programs.²⁴ Knowing the important role played by hyperconjugative interactions on the Fermi contact transmission in vicinal SSCCs, hyperconjugative interactions were evaluated using the natural bond orbital (NBO)²⁵ analysis, implemented in Gaussian03. The B3LYP hybrid functional was used in all calculations, which consists of the hybrid three parameters Becke–Hartree–Fock exchange

Received: August 29, 2011

Revised: November 7, 2011

Published: November 07, 2011

Scheme 1. Compounds Studied in This Work^a

^a 2-X-4-*t*-butylcyclohexanones (1–5) and 2-X-4-*t*-butylcyclohexanols (6–10), where a stands for axial and e for equatorial.

and the Lee–Yang–Parr correlation functionals.²⁶ For geometry optimizations, the aug-cc-pVTZ basis set was chosen.²⁷ Calculations of all four isotropic terms of $^3J_{\text{CH}}$ SSCC, i.e., Fermi contact (FC); spin dipolar (SD); paramagnetic spin orbit (PSO); and diamagnetic spin orbit (DSO), were carried out using the EPR-III basis set²⁸ for H and C and cc-pVDZ for O and halogen atoms. The former basis set is of triple- ζ quality and includes diffuse and polarization functions; its *s* part is enhanced to better reproduce the electronic density in the nuclear regions; this point is particularly important when calculating the FC term.

RESULTS AND DISCUSSION

Table 1 compares the theoretical and experimental $^3J_{\text{C2H6eq}}$ SSCCs for compounds 2-X-4-*t*-butylcyclohexanones (1–5). 2-Me-4-*t*-butylcyclohexanones are included for analyzing the influence of a nonbearing lone pair substituent. It is observed that there is an excellent agreement between theoretical and experimental $^3J_{\text{C2H6eq}}$ SSCCs. For this reason, theoretical data for compounds 2a and 2b, which could not be measured, are considered reliable for this work's purpose. $^3J_{\text{C2H6eq}}$ SSCCs for compounds 3a, 4a, and 5a highlight the influence of the equatorial or axial heteroatom orientation on $^3J_{\text{C2H6eq}}$ SSCCs, which are approximately twice as large as those for the respective *trans* derivatives, 3b, 4b, and 5b. It is highlighted that this effect is not observed in 2a and 2b, i.e., it is evident that this trend, which is by far dominated by the FC term, originates in the orientation of the halogen atom.

Table 2 compares theoretical and experimental $^3J_{\text{C2H6eq}}$ SSCCs for the compounds of 2-X-4-*t*-butylcyclohexanol (6–10) (X = H, Me, F, Cl and Br).

Table 1. Optimized Bond $\text{C}_2\text{—C}_1\text{—C}_6 = \theta$ and Dihedral $\text{C}_2\text{—C}_1\text{—C}_6\text{—H}_{6\text{eq}} = \phi$ Angles (deg); Calculated and Experimental $^3J_{\text{C2H6eq}}$ SSCCs (Hz) and FC (Hz) Terms; X—O Distance (Å) and $\text{C}_2\text{—C}_6$ Distance (Å) for the 2-X-4-*t*-Butylcyclohexanones (X = H, Me, F, Cl, and Br)

compd	θ	ϕ	$^3J_{\text{C2H6eq}}$ theor	$^3J_{\text{C2H6eq}}$ exptl	FC	$d_{\text{X—O}}$	$d_{\text{C2—C6}}$ ^d
1	115.0	172.1	3.10	3.1 ^a	3.11		2.550
2a	114.8	174.3	3.36	<i>b</i>	3.38		2.560
2b	116.0	171.2	2.71	<i>b</i>	2.69		2.576
3a	113.1	175.2	6.10	6.1	6.02	2.687 ^c	2.535
3b	113.8	177.0	2.71	<i>b</i>	2.65	3.309	2.542
4a	112.0	176.1	6.02	6.0	5.95	2.965 ^c	2.529
4b	115.0	172.6	3.30	3.2	3.21	3.541	2.563
5a	112.0	175.7	5.90	5.9	5.75	3.071 ^c	2.527
5b	116.0	170.9	3.49	3.3	3.34	3.635	2.565

^a Taken from ref 5. ^b Could not be measured; 3b could not be observed owing to the overlapping between $\text{H}_{6\text{eq}}$ and $\text{H}_{3\text{eq}}$ signals. ^c The corresponding sum of the X and O van der Waals radii are X = F (1.52 + 1.47) = 2.99 Å; X = Cl (1.52 + 1.75) = 3.27 Å; and X = Br (1.52 + 1.85) = 3.37 Å. ^d In all cases $d_{\text{C1—C6}}$ is shorter than twice the carbon van der Waals radius (3.40 Å) for all substituents and for any of both configurations, i.e., either *cis* or *trans*.

Table 2. Optimized Bond, θ , and Dihedral, ϕ , Angles (deg); Experimental $^3J_{\text{C2H6eq}}$ SSCCs (Hz), Their FC Term (Hz), and the Optimized $d_{\text{X—O}}$ and $d_{\text{C2—C6}}$ Distances (Å) for 2-X-4-*t*-Butylcyclohexanols (X = H, Me, F, Cl, and Br)

compd	θ	ϕ	$^3J_{\text{C2H6eq}}$ theor	$^3J_{\text{C2H6eq}}$ exptl	FC	$d_{\text{X—O}}$	$d_{\text{C2—C6}}$ ^b
6a	110.7	175.0	6.78	6.5	6.83		2.512
6b	110.7	177.5	7.39	7.0	7.45		2.504
7a	110.7	176.3	6.92	<i>a</i>	6.98		2.520
7b	112.0	175.2	6.07	<i>a</i>	6.10		2.539
7c	111.3	177.8	6.92	<i>a</i>	6.99		2.521
7d	112.0	177.9	6.35	<i>a</i>	6.39		2.535
8a	109.5	175.4	10.66	10.5	10.63	2.771	2.489
8b	111.1	175.1	5.35	5.7	5.37	3.568	2.517
8c	109.5	177.7	10.96	11.2	10.93	2.844	2.483
8d	111.1	176.3	6.43	6.4	6.42	2.777	2.513
9a	108.5	176.3	11.66	11.1	11.60	3.091	2.483
9b	111.7	173.7	6.64	<i>a</i>	6.62	4.021	2.530
9c	109.5	177.6	12.06	<i>a</i>	12.00	3.116	2.482
9d	111.7	175.4	7.90	7.6	7.86	3.077	2.528
10a	108.7	176.5	11.95	11.1	11.81	3.216	2.480
10b	112.0	173.4	6.91	<i>a</i>	6.82	4.117	2.533
10c	108.7	177.8	12.42	11.5	12.29	3.229	2.477
10d	111.9	175.2	8.40	8.0	8.29	3.197	2.529

^a Only theoretical values of $^3J_{\text{C2H6eq}}$ were obtained. ^b As observed in the ketone compounds displayed in Table 1, $d_{\text{C1—C6}}$ is notably shorter than twice the C van der Waals radius (3.40 Å).

The FC terms reported in Table 2 are larger than the corresponding values in 2-X-4-*t*-butylcyclohexanones reported in Table 1. The respective θ values as well as $d_{\text{C2—C6}}$ distances are smaller than those reported in Table 1. This is consistent with the assumption made above about the existence of a further FC coupling pathway for transmitting $^3J_{\text{C2H6eq}}$ SSCCs since the $d_{\text{C2—C6}}$ distance is shorter than twice the C van der Waals

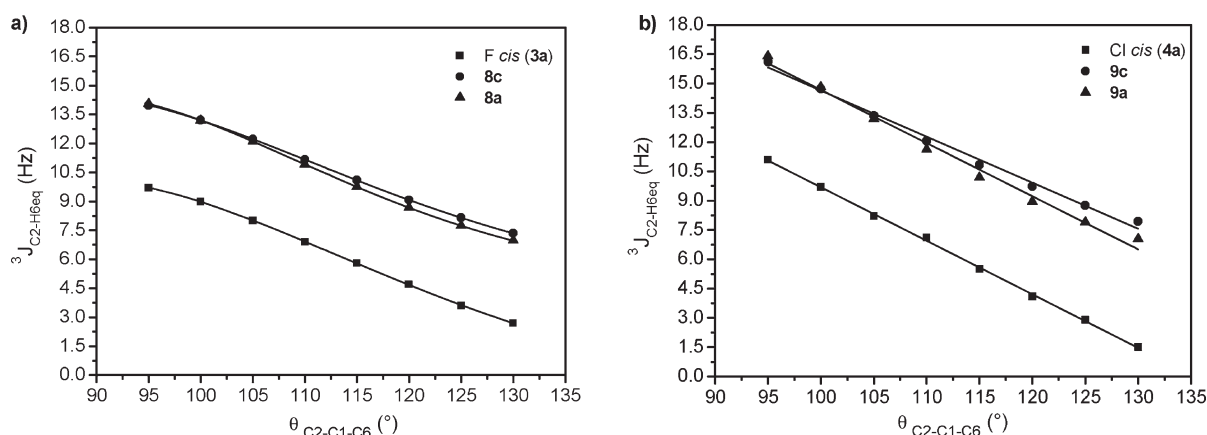


Figure 1. Comparison between plots of $^3J_{C2H6eq}$ SSCC versus θ in *cis*-2-*X*-4-*t*-butylcyclohexanols and *cis*-2-*X*-4-*t*-butylcyclohexanones: (a) $X = F$ and (b) $X = Cl$.

radius, $2 \times 1.70 = 3.40$ Å. This suggests that this coupling pathway is determined by the overlap of the rear lobes of bonds σ_{C2-X} and $\sigma_{C6-H6eq}$; this phenomenon is referred to in the literature as the rear lobes interaction.²⁹ The efficiency of this additional FC coupling pathway depends mainly on the following three factors: (i) the d_{C2-C6} distance; (ii) the relative orientation of the rear lobes of the $\sigma_{C6-H6eq}$ and σ_{C2-X} bonds; and (iii) the extension of the rear lobe of the σ_{C2-X} bond, which strongly depends on the nature of the X atom. In order to further support these rationalizations, $^3J_{C2H6eq}$ SSCC were calculated for different values of $\theta = C2-C1-C6$, changing it in 5° steps, while all other geometrical parameters were allowed to relax.

Figure 1 compares $^3J_{C2H6eq}$ versus θ in ketones and alcohols ($X = F$ and Cl), where it is observed that trends for both types of compounds are quite similar. This is a direct consequence of point (i) quoted above. It is also observed that for fixed θ values, $^3J_{C2H6eq}$ SSCCs in ketones are smaller than for the respective alcohols. This is indicative that point (ii) holds since the different orientations of rear lobes lead to different efficiencies for transmitting the FC term. Point (i) is also supported by observing that $^3J_{C2H6eq}$ SSCC is notably larger when $X = \text{halogen}$ is in the equatorial orientation both for ketones and for alcohols; point (ii) is supported observing that for equatorial isomers, $^3J_{C2H6eq}$ SSCC is larger for $X = \text{halogen}$ than for $X = CH_3$ in both ketones and alcohols.

This trend is observed when comparing plots in Figure 1 with those in Figure 2, the latter corresponding to compounds where X is in the axial position.

However, the effect mentioned in point (iii) is appreciated comparing plots displayed in Figure 1a,b, where it is observed that the rear lobe of σ_{C2-Cl} is more efficient than that of σ_{C2-F} for transmitting the FC term of $^3J_{C2H6eq}$ SSCC.

In 2-*X*-4-*t*-butyl-cyclohexanones, the $^3J_{C2H6eq}$ SSCC dependence on θ is also different for X in axial or equatorial positions. Figure 3 compares $^3J_{C2H6eq}$ SSCC versus θ for *trans*-2-*X*-4-*t*-butyl-cyclohexanones (Figure 3a) and *cis*-2-*X*-4-*t*-butylcyclohexanones (Figure 3b).

For the former, Figure 3a, a different trend is observed for $X = F$. This different trend seems to originate also in the rear lobe interaction effect. In fact, the F electronegativity seems to exert a strong inductive effect on the σ_{C2H2eq} bond, decreasing its rear lobe size, being this effect stronger the smaller the θ angle is. To verify this assumption, the rear lobe overlaps for σ_{C2H2eq} and

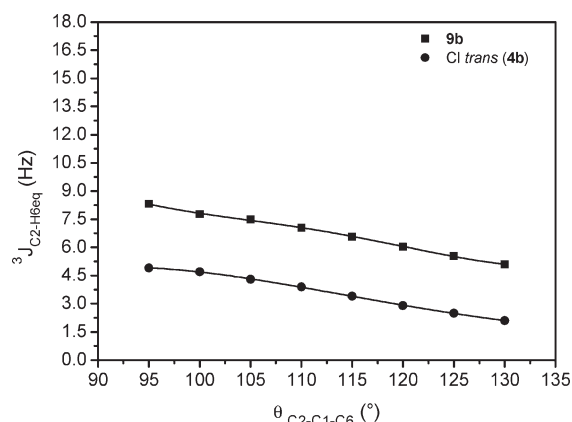


Figure 2. $^3J_{C2H6eq}$ SSCC versus θ for *trans*-2-*Cl*-4-*t*-butylcyclohexanol (9b) and *trans*-2-*Cl*-4-*t*-butylcyclohexanone (4b).

σ_{C6H6eq} were calculated employing the NBO 5.0 program for the three θ values, 130° , 115.2° , and 90° , obtaining, respectively, 61, 37, and 32 in 10^{-4} a.u., although the respective d_{C2-C6} distance decreased from 2.743 to 2.535 and to 2.244 Å. For the latter, Figure 3b in halogenated compounds, a notably stronger dependence than those for $X = H$ and $X = CH_3$ is observed. As noted in Table 1 for *cis* compounds, the $X-O$ distance when $X = F$, Cl , and Br , is notably shorter than the sum of their van der Waals radii, and part of this behavior seems to originate an additional FC coupling pathway owing to the $LP_{2,3}(F)$ and $LP_2(O)$ overlap as described previously¹⁹ for the *syn* isomer in 5-substituted furfurals.

It is interesting to rationalize the notable difference observed in Figure 3b for plots corresponding to compounds with $X = F$, Cl , and Br and those with $X = H$ and CH_3 . Such trends are by far originated in the FC term and as an example $X = Cl$ is chosen. According to data shown in Table 1, for the three *cis*-halogenated ketones, the $X-O$ distance is shorter than the respective sums of their van der Waals radii. Therefore, it is expected that, when decreasing θ , due to an orientation effect of the O and X lone-pairs, they overlap to a larger extent. Table 3 displays (4a) how some NBO parameters are affected by the close proximity between the O and Cl atoms. For instance, an increase in the $LP_3(Cl)/LP_{1,2}(O)$ overlap enhances notably the $LP_1(O) \rightarrow \sigma^*_{C2-C1}$ and $LP_2(O) \rightarrow \sigma^*_{C2-C1}$ hyperconjugative interactions.

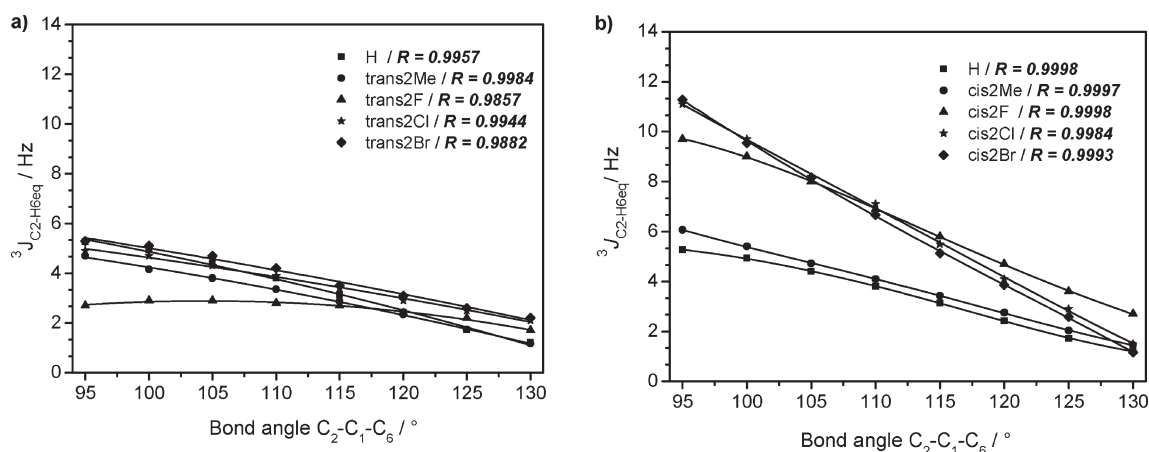


Figure 3. Comparison of $^3J_{C2H6eq}$ versus θ in (a) *trans*-2-X-4-*t*-butylcyclohexanones and (b) *cis*-2-X-4-*t*-butylcyclohexanones (X = H, Me, F, Cl, and Br).

Table 3. In 4a, the Close Proximity between the O and C1 Lone Pairs Affects the Energy of the Hyperconjugative Interactions (in kcal mol⁻¹) Involving Such Lone Pairs

interactions	$\theta = 90^\circ$	$\theta = 110^\circ$	$\theta = 130^\circ$
LP ₁ (O) \rightarrow σ^*_{C2-C1}	4.52	3.14	1.97
LP ₁ (O) \rightarrow σ^*_{C6-C1}	3.99	3.18	2.02
LP ₂ (O) \rightarrow σ^*_{C2-C1}	28.48	25.65	20.31
LP ₂ (O) \rightarrow σ^*_{C6-C1}	27.23	21.76	16.68

Similar hyperconjugative interaction enhancements by steric effects are known in the current literature.^{20,30}

To rationalize the effect of the enhancement of such hyperconjugative interactions on the FC transmission of $^3J_{C2H6eq}$ SSCC, a qualitative analysis described in recent papers^{31,32} is employed. Here, this approach is briefly described before applying it to rationalize such effects. However, before presenting that brief description the following points are highlighted. To discuss results obtained with this approach, some ad hoc expressions are coined, and besides, this description departs somewhat from some standard terminology. Example of the former is our frequently common usage of terms like perturbators and descriptors. An example of the latter is the meaning ascribed here to FC coupling pathways, which intends to stress what are the most common mechanisms for transmitting the FC term (which coincide with those of the Fermi hole), i.e., (a) when two proximate electronic clouds overlap, then exchange interactions take place, and both the FC and the Fermi hole are transmitted; (b) if within a molecular system (monomer, dimer, etc) charge transfer interactions take place (commonly known as conjugative and/or hyperconjugative interactions), they transmit both the FC and the Fermi hole. Within a molecular orbital description, charge transfer interactions mean that electrons are shared by two different orbitals. This is an excellent means for transmitting the spin information associated to the FC term. In the present description effects (a) and (b) define different coupling pathways for transmitting the FC term of a given SSCC. For instance, an example of the (a) class is the rear lobe interaction. Examples of the (b) class were given in several previous papers. An adequate example is the geminal $^2J_{HH}$ SSCC in formaldehyde, one of them is H–C–H, and a second one is given by both LP₂(O) \rightarrow (C–H)* very strong hyperconjugative interactions, i.e., the electrons

within the LP₂(O) nonbonding electron pair are shared with such orbitals.

The FC contribution to $^3J_{C2H6eq}$ SSCC is expanded in terms of contributions from pairs of occupied, *i* and *j*, and virtual, *a* and *b*, molecular orbitals, MOs, in eq 1

$$^3J_{C2H6eq}^{FC} = \Omega^{FC} \sum_{ia,jb} J_{ia,jb}^{FC}(C_2, H_{6eq}) \quad (1)$$

where Ω^{FC} is a constant involving the coupling nuclei magnetogyric ratios as well as universal and numerical constants. As shown previously,³³ MO contributions in eq 1 can be written as those in eq 2

$$^3J_{ia,jb}^{FC}(C_2, H_{6eq}) = ^3W_{ia,jb} [U_{ia,C2}^{FC} U_{jb,H6eq}^{FC} + U_{ia,H6eq}^{FC} U_{jb,C2}^{FC}] \quad (2)$$

where $^3W_{ia,jb} = (^3A + ^3B)_{ia,jb}^{-1}$ are the elements of the inverse of the triplet Polarization Propagator matrix, PP. Matrices 3A and 3B can be written in terms of bielectronic molecular integrals. $U_{ia,C2}^{FC}$ ($U_{jb,H6eq}^{FC}$) are the matrix elements of the FC operator between the occupied *i* (*j*) and virtual *a* (*b*) MOs evaluated at the C₂ (H_{6eq}) site of each coupling nuclei, eq 3, where $\delta(\vec{r}_N)$ is the Dirac's delta function. It corresponds to the overlap between *i* and *a* MOs at the site of the *N* nucleus and are designated as perturbators.

$$U_{ia,N}^{FC} = \langle i | \delta(\vec{r}_N) | a \rangle \text{ where } N = C_2, H_{6eq} \quad (3)$$

Equation 2 expresses each term of eq 1 as a product between the PP term and the perturbators as given in eq 3; the latter corresponds to the overlap between occupied MO *i* and vacant MO *a* at the site of each coupling nuclei. It is important to obtain an estimation of that overlap without forgetting that this qualitative approach is intended for narrowing the present gap between visions expressed by pure experimental oriented and pure theoretical oriented molecular scientists working in any field. For this last reason this qualitative analysis is carried out resorting only to software well-known in the current literature. It is recalled that eqs 1–3 are invariant under unitary transformations. For these reasons, it can be assumed that in eq 3 molecular orbitals are localized, LMOs, intending to reproduce the common chemical functions like bonds, lone pairs, and core orbitals for occupied LMOs and antibonding orbitals for unoccupied

Table 4. Relevant Parameters for Estimating $D_{ia,jb}$ for $\theta = 90^\circ$, 110° , and 130° in **4a**

occupancies	$\theta = 90^\circ$	$\theta = 110^\circ$	$\theta = 130^\circ$
$\sigma_{C6-H6eq}$	1.974	1.978	1.969
$\sigma^*_{C6-H6eq}$	0.016	0.011	0.010
σ_{C2-C1}	1.975	1.978	1.984
σ^*_{C2-C1}	0.114	0.100	0.085
$LP_2(O)$	1.835	1.873	1.899
$LP_3(Cl)$	1.972	1.873	1.970
s % character at C_2	27.55	28.09	27.44
$D_{ia,jb}$ (eq 4)	5.4	3.7	2.5

LMOs. It is highlighted that each term in eqs 2 and 3 is not invariant under unitary transformations; however, this fact does not affect the basic ideas underlined in this approach. In fact, this analysis is only qualitative and an adequate choice of LMOs is made as pointed out below.

It should be noted that the right-hand side of eq 2 can be interpreted as follows: the two coupling nuclei can be considered as the emitting and the receiving nucleus of the FC spin information. Since always ${}^nJ_{AB} = {}^nJ_{BA}$, any of them can play any of these two roles. Within this schematic description, the inverse of the triplet PP matrix 3W describes how such FC spin information can be transmitted by the whole molecular electronic system from the emitting to the receiving nuclei. The term in square brackets describes the ability of the electronic clouds surrounding each coupling nuclei for capturing such spin information. Different SSCC trends like those displayed in Figure 3b can originate on changes either of the PP term or on the perturbators, or in both types of terms simultaneously.

Taking into account the above considerations, the overlaps quoted in eq 3 can be taken as the product of the s % character of i and a LMOs at the site of the coupling nucleus N . However, to be consistent with the ideas presented above, NBO's as given by Weinhold et al.²⁵ are chosen as those LMOs. Recalling that eqs 1–3 are only considered qualitatively, and noting that these orbitals are closely related to chemical properties, the lack of invariance under unitary transformations affecting each term of eq 2 is nicely overcome. However, this choice presents the following problem: a bonding and its antibonding orbital have the same s % character at the sites of both nuclei of such bond. Therefore, further simplifications are introduced in eq 3, scaling the s % character of each orbital with its occupation number. This can be considered as the effective s % degree of that orbital. This approximate value of each perturbator is dubbed now as its descriptor, and its expression is given by eq 4. With such descriptors, it is possible to detect if the main trend of a given SSCC is mainly given by the perturbators trend or by the PP trend.

The O and Cl lone pair's important interaction seems to activate additional coupling pathways for transmitting the FC information between the C_2 and H_{6eq} nuclei. The interaction between $LP_{1,2}(O)$ and $LP_3(Cl)$ should affect not only the perturbators in eq 2 but also the corresponding 3W term. To verify this last assertion, the influence of perturbators, eq 2, on trends displayed in Figure 3b. the approximations described in previous papers³² and summarized above are introduced in eqs 1–3.

When dealing with the ${}^3J_{C2H6eq}$ SSCC eq 2, the ${}^3W_{ia,ia}$ diagonal terms are multiplied by very small perturbators and, therefore,

Table 5. Hyperconjugative Interactions Involving the Carbonyl π -Electronic System Defining a Homoallylic-Like Coupling Pathway for the FC Term of ${}^3J_{C2H6eq}$ SSCC^a

donor	acceptor	HI	back donation	sum
$\theta = 130^\circ$				
σ_{C1-Cl2}	$\pi^*_{C=O}$	0.95	0.94	1.89
σ_{C1-C6}	$\pi^*_{C=O}$	0.64	0.96	1.60
$\sigma_{C1-H1ax}$	$\pi^*_{C=O}$	6.33	2.01	8.24
$\sigma_{C6-H6eq}$	$\pi^*_{C=O}$	2.38		2.38
$\theta = 125^\circ$				
σ_{C1-C6}	$\pi^*_{C=O}$	1.44	0.80	2.24
$\sigma_{C1-H1ax}$	$\pi^*_{C=O}$	6.42	2.20	8.62
$\sigma_{C6-H6eq}$	$\pi^*_{C=O}$	1.06		1.06
$\theta = 120^\circ$				
σ_{C1-C6}	$\pi^*_{C=O}$	1.79	0.96	2.75
$\sigma_{C1-H1ax}$	$\pi^*_{C=O}$	6.24	2.08	8.32
$\sigma_{C6-H6eq}$	$\pi^*_{C=O}$	0.53		0.53
$\theta = 115^\circ$				
σ_{C1-C6}	$\pi^*_{C=O}$	2.18	1.10	3.28
$\sigma_{C1-H1ax}$	$\pi^*_{C=O}$	5.78	1.91	7.69
$\sigma_{C6-H6eq}$	$\pi^*_{C=O}$			

^a For smaller angles, this contribution is below the NBO program threshold.

only nondiagonal terms of the 3W matrix yield important contributions. Since only 3W diagonal matrix elements depend explicitly on the vacant-occupied energy gap of each pair of vacant-occupied orbitals, they are not taken into account in this qualitative analysis.

The main perturbator term in eq 2 corresponds to orbitals: $i = \sigma_{C2-C1}$; $a = \sigma^*_{C2-C1}$; $j = \sigma_{C6-H6eq}$; and $b = \sigma^*_{C6-H6eq}$ and a descriptor of the square bracket factor in eq 2 for values of $\theta = 90^\circ$, 110° , and 130° can be expressed as in eq 4, always recalling that this estimation is only valid to compare perturbators in analogous SSCCs. This estimation is dubbed as a descriptor, eq 4, for the perturbator under consideration.

$$D_{ia,jb} = [O_{cc}(\sigma_{C2-C1})][s\%C(\sigma_{C2-C1})]^2 [O_{cc}(\sigma^*_{C2-C1})] \times [O_{cc}(\sigma_{C6-H6eq})][O_{cc}(\sigma^*_{C6-H6eq})] \quad (4)$$

where the s % character at H_{6eq} in the $\sigma_{C6-H6eq}$ bond differs in a negligible amount from 100% (99.96, 99.96, and 99.95) for (**4a**) and $\theta = 90^\circ$, 110° , and 130° , respectively; therefore, it is not included in eq 4. Table 4 displays the relevant data for calculating the descriptors $D_{ia,jb}(\theta = 90^\circ)$, $D_{ia,jb}(\theta = 110^\circ)$ and $D_{ia,jb}(\theta = 130^\circ)$. It is observed that decreasing θ from 130° to 90° yields an increase for the FC term of ${}^3J_{C2H6eq}$ SSCC from 1.5 to 12.2 Hz, while the corresponding perturbator descriptor increases only from 2.5 to 5.4. This indicates that there should be a significant increase in the efficiency for transmitting that coupling from the emitting to the receiving nuclei, which within this approach originates in an increase of the 3W matrix element.

This supports the assumption made above that a decrease in θ activates additional coupling pathways. By recalling that hyperconjugative interactions behave like carriers of the spin information associated to the FC interaction,^{34,35} it is easy to observe the following additional coupling pathway $\sigma_{C6-H6eq} \rightarrow \pi^*_{C1=O}/\sigma_{C2-Cl2} \rightarrow \pi^*_{C1=O}$; see Table 5. This is similar to that of

Table 6. For Compound (4a), Hyperconjugative Interactions (kcal mol⁻¹) Contributing to the sequence: I = $\sigma_{C2-Cl2} \rightarrow \sigma_{C1-C6} + \sigma_{C1-C6} \rightarrow \sigma_{C2-Cl2}^*$; II = $LP_{1,2}(O) \rightarrow \sigma_{C1-C6}^*$; III = $LP_{1,2}(O) \rightarrow \sigma_{C1-C2}^*$

θ	I	II	III
90°	8.96	31.22	33.00
110°	6.11	23.84	28.79
130°	4.43	22.88	24.94

homoallylic $^4J_{CH}$ SSCCs,³⁶ and therefore, it should correspond to a negative contribution. It becomes, in absolute value, negligibly small for $\theta < 120^\circ$.

Another additional FC coupling pathway has already been mentioned above when discussing Figure 3. This pathway, which is similar to that discussed previously¹⁹ for $^2J_{C1,Hf}$ SSCCs in *syn* rotamers of 5-X-furfurals, originates mainly in the overlap of $LP_{1,2}(O)$ and $LP_{2,3}(Cl)$ lone pairs in compound 4a. This enhances the efficiency for transmitting the FC spin information corresponding to $^3J_{C2H6eq}$ SSCC by increasing the 3W factor in eq 2. By considering hyperconjugative interactions as carriers of that spin information (or of the Fermi hole), it is easy to obtain a pictorial representation of how such term is enhanced due to the strong interaction between O and Cl lone pairs, which affects the following concatenated sequence of hyperconjugative interactions, called the sequence: $\sigma_{C2-Cl2} \rightarrow \sigma_{C1-C6}^* / \sigma_{C1-C6} \rightarrow \sigma_{C2-Cl2}^*$; $LP_{1,2}(O) \rightarrow \sigma_{C1-C6}^*$; $LP_{1,2}(O) \rightarrow \sigma_{C1-C2}^*$. In fact, the first two carry the C_2 spin information into the σ_{C1-C6} bond/antibond system, and the latter two bring that information back to the bond/antibond σ_{C2-Cl2} system. Table 6 shows the collected values of such interactions when increasing θ from 90° to 130°, i.e., they increase monotonically following the same trend like plots in Figure 3b for halogenated *cis*-2-X-4-*t*-butylcyclohexanones.

CONCLUSIONS

Differences between $^3J_{C2H6eq}$ SSCCs in 2-X-4-*t*-butyl-cyclohexanone (X = H, CH₃, F, Cl, and Br) and in their alcohol derivatives are rationalized in terms of their respective FC contributions. For either axial or equatorial X orientations, such SSCCs are larger in the latter than in the former series. That trend is rationalized as originating mainly in the rear lobe interaction, i.e., in the FC transmission owing to exchange interactions taking place in the region where the $\sigma_{C2-X2eq}$ and $\sigma_{C6-H6eq}$ rear-lobes overlap for X with equatorial orientation. Similarly, for X with an axial orientation, exchange interactions take place in the region where $\sigma_{C2-H2eq}$ and $\sigma_{C6-H6eq}$ rear lobes overlap. The very good agreement found between calculated and experimental $^3J_{C2H6eq}$ SSCCs allowed us to obtain insight into those trends by studying $^3J_{C2H6eq}$ SSCCs versus θ , i.e., the $C_2-C_1-C_6$ angle. Three main factors defining the above-mentioned rear lobe interactions are observed, namely, (i) the C_2-C_6 distance; (ii) the relative rear-lobe orientations; and (iii) the rear lobe size. This latter effect was estimated by observing the different effect on $^3J_{C2H6eq}$ SSCCs for X = F and Cl in the equatorial orientation.

From Figure 3, it is observed in ketones for X in the equatorial orientation that there is an additional increase in $^3J_{C2H6eq}$ SSCC when X = halogen. Resorting to a qualitative approach presented previously, this effect was rationalized mainly in terms of an

additional coupling pathway activated by the interaction between $LP_{1,2}(O)$ and $LP_{2,3}(X)$ lone pairs.

AUTHOR INFORMATION

Corresponding Author

*E-mail: tormena@iqm.unicamp.br.

ACKNOWLEDGMENT

We are grateful to FAPESP (grant 10/10993-9) for the financial support of this work and to the fellowship to L.C.D. (grant 10/15765-4) and CNPq for a scholarship to D.C.F and fellowship to C.F.T. Financial support from CONICET (PIP 0369/10) and UBATEC (X047) to R.H.C. are gratefully acknowledged.

REFERENCES

- (1) Karplus, M. *J. Chem. Phys.* **1959**, *30*, 11.
- (2) Karplus, M. *J. Phys. Chem.* **1960**, *64*, 1793.
- (3) Karplus, M. *J. Am. Chem. Soc.* **1963**, *85*, 2870.
- (4) Thomas, W. A. *Prog. Nucl. Magn. Reson. Spectrosc.* **1997**, *30*, 183.
- (5) Parella, T.; Sánchez-Ferrando, F.; Virgili, A. *Magn. Reson. Chem.* **1992**, *14*, 657.
- (6) Liu, M.; Farran, R. D.; Gillam, J. M.; Nicholson, J. K.; Linton, J. C. *J. Magn. Reson.* **1995**, *109*, 275.
- (7) Köver, K. E. *J. Magn. Reson.* **2006**, *181*, 89.
- (8) dos Santos, F. P.; Tormena, C. F.; Contreras, R. H.; Rittner, R.; Magalhães, A. *Magn. Reson. Chem.* **2008**, *46*, 107.
- (9) San-Fabián, J.; Guilleme, J.; Díez, E.; Lazzeretti, P.; Malagoli, M.; Zanasi, R.; Mora, A. L. *Mol. Phys.* **1994**, *82*, 913.
- (10) Guilleme, J.; San-Fabián, J.; Díez, E. *Mol. Phys.* **1997**, *91*, 243.
- (11) San-Fabián, J.; Guilleme, J.; Díez, E. *Av. Quím.* **1995**, *91*, 200.
- (12) Barfield, M.; Smith, W. B. *J. Am. Chem. Soc.* **1992**, *114*, 1574.
- (13) Smith, W. B.; Barfield, M. *Magn. Reson. Chem.* **1993**, *31*, 696.
- (14) VanWijk, J.; Huckriede, B. D.; Ippel, J. H.; Altona, C. *Methods Enzymol.* **1992**, *211*, 286.
- (15) Löhr, F.; Schmidt, J. M.; Rüterjans, H. *J. Biomol. NMR* **1999**, *14*, 1.
- (16) Barone, V.; Peralta, J. E.; Contreras, R. H. *J. Comput. Chem.* **2001**, *22*, 1615.
- (17) Contreras, R. H.; Suardiáz, R.; Pérez, C.; Crespo-Otero, R.; San Fabián, J.; García de la Vega, J. M. *J. Chem. Theory Comput.* **2008**, *4*, 1494.
- (18) Contreras, R. H.; Suardiáz, R.; Pérez, C.; Crespo-Otero, R.; San Fabián, J.; García de la Vega, J. M. *Int. J. Quantum Chem.* **2010**, *110*, 532.
- (19) Pérez, C.; Suardiáz, R.; Ortiz, P. J.; Crespo-Otero, R.; Bonetto, G. M.; Gavín, J. A.; García de la Vega, J. M.; San Fabián, J.; Contreras, R. H. *Magn. Reson. Chem.* **2008**, *46*, 846.
- (20) Contreras, R. H.; Peralta, J. E. *Prog. Nucl. Magn. Reson. Spectrosc.* **2000**, *37*, 321.
- (21) (a) Vitorge, M. C.; Chenon, M. T.; Couprie, C.; Lumbroso-Bader, N. *Org. Magn. Reson.* **1983**, *21*, 20. (b) Contreras, R. H.; Natiello, M. A.; Tufro, M. F.; De Kowalewski, D. G.; Scuseria, G. E. *Z. Phys. Chem.* **1986**, *267*, 289.
- (22) Nolis, P.; Espinosa, J. F.; Parella, T. *J. Magn. Reson.* **2006**, *180*, 39.
- (23) Sychrovský, V.; Gräfenstein, J.; Cremer, D. *J. Chem. Phys.* **2000**, *113*, 3530.
- (24) Frisch, M. J.; Trucks, G. W.; Schlegel, H. B.; Scuseria, G. E.; Robb, M. A.; Cheeseman, J. R.; Montgomery, J. A., Jr.; Vreven, T.; Kudin, K. N.; Burant, J. C.; Millam, J. M.; Iyengar, S. S.; Tomasi, J.; Barone, V.; Mennucci, B.; Cossi, M.; Scalmani, G.; Rega, N.; Petersson, G. A.; Nakatsuji, H.; Hada, M.; Ehara, M.; Toyota, K.; Fukuda, R.; Hasegawa, J.; Ishida, M.; Nakajima, T.; Honda, Y.; Kitao, O.; Nakai, H.; Klene, M.; Li, X.; Knox, J. E.; Hratchian, H. P.; Cross, J. B.; Bakken, V.; Adamo, C.; Jaramillo, J.; Gomperts, R.; Stratmann, R. E.; Yazyev, O.

Austin, A. J.; Cammi, R.; Pomelli, C.; Ochterski, J. W.; Ayala, P. Y.; Morokuma, K.; Voth, G. A.; Salvador, P.; Dannenberg, J. J.; Zakrzewski, V. G.; Dapprich, S.; Daniels, A. D.; Strain, M. C.; Farkas, O.; Malick, D. K.; Rabuck, A. D.; Raghavachari, K.; Foresman, J. B.; Ortiz, J. V.; Cui, Q.; Baboul, A. G.; Clifford, S.; Cioslowski, J.; Stefanov, B. B.; Liu, G.; Liashenko, A.; Piskorz, P.; Komaromi, I.; Martin, R. L.; Fox, D. J.; Keith, T.; Al-Laham, M. A.; Peng, C. Y.; Nanayakkara, A.; Challacombe, M.; Gill, P. M. W.; Johnson, B.; Chen, W.; Wong, M. W.; Gonzalez, C.; Pople, J. A. *Gaussian 03*, revision E.01; Gaussian, Inc.: Wallingford, CT, 2004.

(25) Glendening, E. D.; Badenhoop, J. K.; Reed, A. E.; Carpenter, J. E.; Bohmann, J. A.; Morales, C. M.; Weinhold, F. *NBO 5.0G*; Theoretical Chemistry Institute, University of Wisconsin: Madison, WI, 2001; <http://www.chem.wisc.edu/~nbo5/>, program as implemented in the Gaussian03 package.

(26) (a) Becke, A. D. *Phys. Rev. A* **1988**, 38, 3098. (b) Becke, A. D. *J. Chem. Phys.* **1993**, 98, 5648. (c) Lee, C. T.; Yang, W. T.; Parr, R. G. *Phys. Rev. B* **1988**, 37, 785.

(27) Woon, D. E.; Dunning, T. H. *J. Chem. Phys.* **1993**, 98, 1358.

(28) Barone, V. *J. Chem. Phys.* **1994**, 10, 6834.

(29) Marshall, J. L.; Walter, S. R.; Barfield, M.; Marchand, A. P.; Segré, A. L. *Tetrahedron* **1976**, 32, 537.

(30) Cheng, M.; Pu, X.; Wang, N.-B.; Li, M.; Tian, A. *New J. Chem.* **2008**, 32, 1060.

(31) Anizelli, P. R.; Favaro, D. C.; Contreras, R. H.; Tormena, C. F. *J. Phys. Chem. A* **2011**, 115, 5684.

(32) Vilcachagua, J. D.; Ducati, L. C.; Rittner, R.; Contreras, R. H.; Tormena, C. F. *J. Phys. Chem. A* **2011**, 115, 7762 and references cited therein.

(33) (a) Oddershede, J. Polarization Propagator Calculations. In *Advances in Quantum Chemistry*; P.-O. Löwdin, Ed.; Elsevier: New York, **1978**; Vol. 11, p 272. (b) Diz, A. C.; Giribet, C. G.; Ruiz de Azúa, M. C.; Contreras, R. H. *Int. J. Quantum Chem.* **1990**, 37, 663. (c) Electronic origin of high resolution NMR parameters. Contreras, R. H.; Giribet, C. G.; Ruiz de Azúa, M. C.; Ferraro, M. B. *Studies in Physical and Theoretical Chemistry*. In *Structure, Interactions and Reactivity*; Fraga, S., Ed.; Elsevier: New York, 1992; Vol. 77B, Chapter 7, p 212. (d) Contreras, R. H.; Ruiz de Azúa, M. C.; Giribet, C. G.; Aucar, G. A.; Lobayan de Bonczok, R. *J. Mol. Struct. (Theochem)* **1993**, 284, 249. (e) Giribet, C. G.; Ruiz de Azúa, M. C.; Contreras, R. H.; Lobayan de Bonczok, R.; Aucar, G. A.; Gomez, S. *J. Mol. Struct. (Theochem)* **1993**, 300, 467.

(34) Contreras, R. H.; Esteban, A. L.; Diez, E.; Head, N. J.; Della, E. W. *Mol. Phys.* **2006**, 104, 485.

(35) Contreras, R. H.; dos Santos, F. P.; Ducati, L. C.; Tormena, C. F. *Magn. Reson. Chem.* **2010**, 48, S151.

(36) Barfield, M.; Chakrabarty, B. *Chem. Rev.* **1969**, 69, 757.